Nuclear Engineering and Design 443 (2025) 114259

Contents lists available at ScienceDirect

Nuclear Engineering and Design

journal homepage: www.elsevier.com/locate/nucengdes

Sensitivity analysis of a flow redistribution model for a multidimensional and multifidelity simulation of fuel assembly bow in a pressurized water reactor

Ali Abboud [a,b,*], Stanislas de Lambert [b], Josselin Garnier [a], Bertrand Leturcq [b], Nicolas Lamorte [c]

[a] CMAP, CNRS, École polytechnique, Institut Polytechnique de Paris, 91120 Palaiseau, France
[b] Université Paris-Saclay, CEA, Service d'Études Mécaniques et Thermiques, 91191, Gif-sur-Yvette, France
[c] Framatome, 2 rue du Professeur Jean-Bernard, 69007 Lyon, France

ARTICLE INFO

Keywords:
Fuel assembly bow
Thermal hydraulic
Uncertainty quantification
Surrogate modeling
Sensitivity analysis

ABSTRACT

In the core of nuclear reactors, fluid–structure interaction and intense irradiation lead to progressive deformation of fuel assemblies. When this deformation is significant, it can lead to additional costs and longer fuel unloading and reloading operations. Therefore, it is preferable to adopt a fuel management that avoids excessive deformation and interactions between fuel assemblies. However, the prediction of deformation and interactions between fuel assemblies is uncertain. Uncertainties affect neutronics, thermohydraulics and thermomechanics parameters. Indeed, the initial uncertainties are propagated over several successive power cycles of twelve months each through the coupling of non-linear, nested and multidimensional thermal–hydraulic and thermomechanical simulations. In this article, we set out to study the hydraulic contribution and quantify the associated uncertainty. To achieve this objective, we develop a multi-stage approach to carry out an initial sensitivity analysis, highlighting the most influential parameters in the hydraulic model. By optimally adjusting these parameters, we aim to obtain a more accurate description of the flow redistribution phenomenon in the reactor core. The aim of the sensitivity analysis presented in this article is to construct an accurate and suitable surrogate model that represents the in-core lateral hydraulic forces in a given state. This surrogate model could then be coupled with a thermomechanical model to quantify the final uncertainty in the simulation of fuel assembly bow within a pressurized water reactor. This approach will provide a better understanding of the interactions between hydraulic and thermomechanical phenomena, thereby improving the reliability and accuracy of the simulation results.

1. Introduction

1.1. Industrial issue

The rapid insertion of control rod clusters is of crucial importance for safety, as it allows for the quick reduction or immediate shutdown of the reactor power, ensuring control of reactivity, which is one of the fundamental safety functions during operation situations. Since the 1990s, several incidents of incomplete insertion of control rods have occurred, potentially jeopardizing this safety function. The first event took place in 1994 in the Ringhals 4 reactor, when a control rod failed to fully insert after an emergency reactor shutdown, root cause investigation showed that the incomplete rod insertion (IRI) was caused by increased friction between the control rod and the assemblies guide thimbles (Andersson et al., 2005). In other words, the control rods slide within the guide tubes, and when the assembly is deformed, the guide tubes are deformed in the same manner, resulting in friction between the guide tubes and the control bars, preventing their complete insertion. In the following years, several other incidents of incomplete control rod insertion and increased control rod insertion times were detected in various Western reactors (Roudier and Béraha, 1996). In German pressurized water reactors, increased permanent deformations of fuel assemblies have been observed since the year 2000 (RSK, 2015). Both the extent of deformations and the frequency of occurrences had increased since then until the early 2010s, when several events related to fuel assemblies deformation were reported in different nuclear power plants. In a unique case, an incident of incomplete control rod insertion occurred. In several other cases, increased control rod insertion times were measured, exceeding the specified maximum values. In most of the mentioned cases, a collective deformation of fuel assemblies across the entire core was observed. Individual fuel assemblies can exhibit deflections reaching up to around 20 mm and are generally deformed into one of the three characteristic shapes, namely C, S and W (see Fig. 1).

* Corresponding author at: Université Paris-Saclay, CEA, Service d'Études Mécaniques et Thermiques, 91191, Gif-sur-Yvette, France.
E-mail address: ali.abboud@cea.fr (A. Abboud).

https://doi.org/10.1016/j.nucengdes.2025.114259
Received 23 September 2024; Received in revised form 18 June 2025; Accepted 19 June 2025
Available online 14 July 2025
0029-5493/© 2025 The Authors. Published by Elsevier B.V. This is an open access article under the CC BY license (http://creativecommons.org/licenses/by/4.0/).

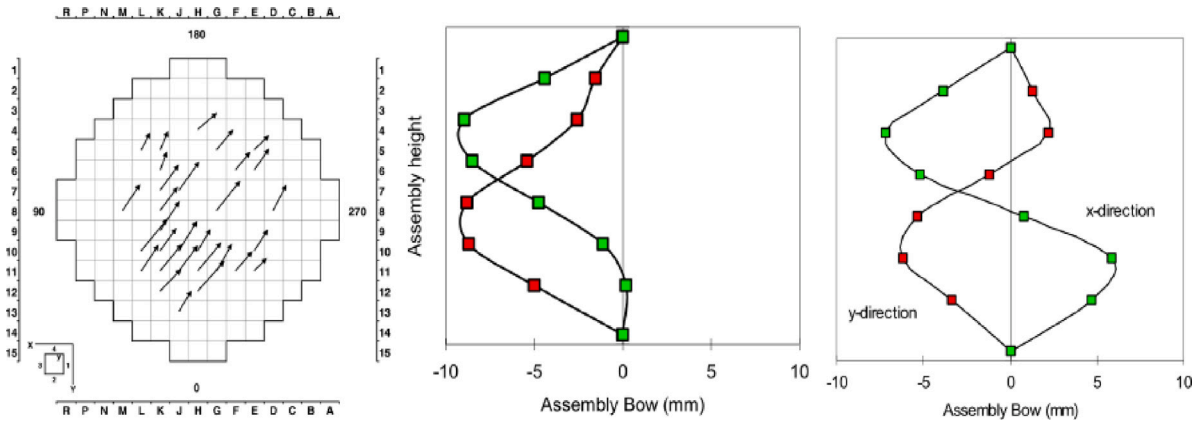

Fig. 1. Collective deformation of fuel assemblies measured at Ringhals 2 (left), C-shaped deformations measured at Ringhals 3 (middle), and S-shaped deformations measured at Ringhals 4 (right).
Source: From Andersson et al. (2005).

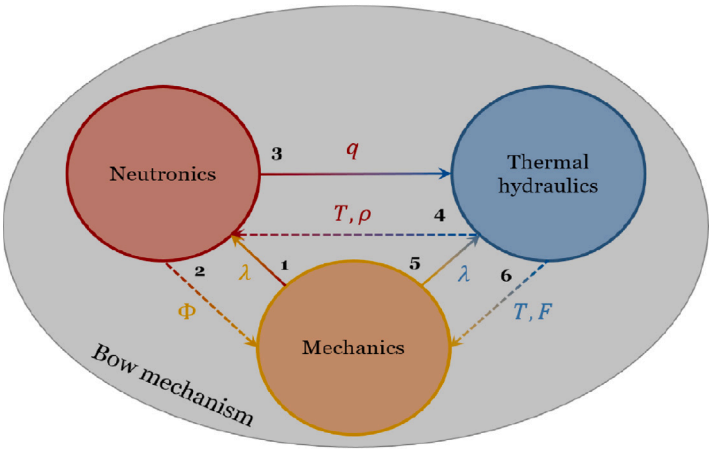

Fig. 2. Physical interactions during the deformation of the assembly.
Source: From De lambert des champs de morel (2021).

1.2. Bow influencing mechanisms

Over the years, a multitude of mechanisms (see Fig. 2) have been discussed as the origins of fuel assembly bow or as factors that promote it. In general, two types of mechanisms influencing deformation must be distinguished: inducing mechanisms and reinforcing mechanisms (Wanninger, 2018). Inducing mechanisms are those that initiate deformation by creating bending moments within the structure. Reinforcing mechanisms are those that cannot cause deformation by themselves but significantly influence how it occurs and at what rate. The final deformation patterns are likely the result of the interaction between different mechanisms, making it difficult to determine and quantify the contribution of each individual effect. This coupling of multiple mechanisms, along with the mechanical coupling of fuel assemblies within the reactor core, can potentially lead to counter-intuitive and self-amplifying effects, possibly explaining the emergence of heavily deformed cores with asymmetric deformation patterns. The main mechanisms influencing the deformation of fuel assemblies are mentioned for instance in Wanninger (2018), Lamorte et al. (2021), Lascar et al. (2015), and De lambert des champs de morel (2021), and they can be summarized as follows: Hold down forces, structural growth, structural creep, fuel assembly stiffness, grid spring relaxation, lateral mechanical coupling, fast neutron irradiation, and lateral hydraulic forces. The simulation of fuel assembly bow throughout power cycles is generally performed with thermomechanical–thermohydraulic coupling (Wanninger, 2018; Lamorte et al., 2021; Lascar et al., 2015; Horváth and Dressel, 2013; de Lambert et al., 2023).

1.3. Literature review on uncertainty quantification in the context of fuel assembly bow and motivation for our work

In exploring existing literature, we observed that the majority of studies focusing on uncertainty quantification are situated within a specific framework centered around phenomena contributing to fuel assembly deformation, or those influencing it, rather than the simulation of the deformation phenomenon itself. Many works address the uncertainty associated with neutron flux calculations, such as Laura Clouvel's thesis in 2019 (Clouvel, 2019). Furthermore, sources of uncertainty related to grid-to-rod fretting, which is the subject of Pernice's research in 2012 (Pernice, 2012), are also discussed, given that grid-to-rod fretting and penetration are the primary causes of fuel failure in pressurized water reactors. However, Wanninger conducted more extensive sensitivity and uncertainty analysis in 2018 (Wanninger, 2018) to assess the model's reactivity to various influencing mechanisms. Sensitivity analysis work in the context of phenomena contributing to fuel assembly deformation, particularly concerning hydraulic calculations, was carried out by de Lambert (de Lambert et al., 2021).

According to what has been discussed in the literature, it is evident that considering uncertainties during the numerical simulation of assembly bow is of crucial importance. However, previous works have mainly sought to highlight this importance, but their results remain limited and highly focused on particular objectives. Our work aims to overcome these limitations by focusing on quantifying uncertainties that propagate through a nonlinear thermohydraulic and

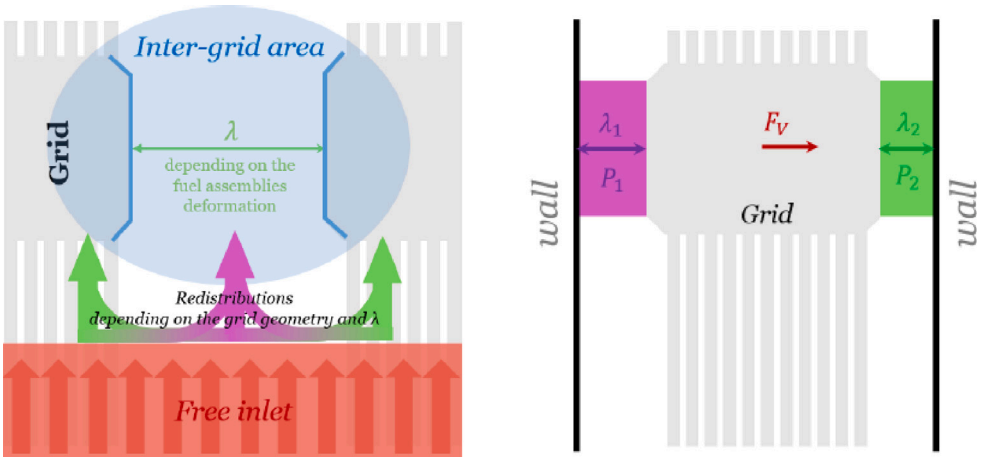

Fig. 3. Local flow redistribution in the core (left), lateral hydraulic force due to a pressure difference around a grid (right).
Source: From De lambert des champs de morel (2021).

thermomechanical coupling. The central idea is to develop an efficient methodology capable of adapting to the multidimensional and multiphysics nature of this simulation, as well as the associated multifidelity approach. In other words, our main objective is to propose a methodological framework that addresses these challenges.

1.4. Summary of the objectives of this article

As mentioned, this work aims at better quantifying uncertainties propagating through the fluid–structure coupling regarding fuel assembly bow. In this article, we present a study regarding the hydraulic contribution – hydraulic forces – to the deformation. It is a first necessary step to a more global framework presented above. Specifically, our work is divided into several parts aiming to deepen our understanding of the flow simulations performed with a dedicated tool and the estimation of forces applied on mechanics. Section 2 is devoted to an initial investigation: evaluating the spatial propagation of local deformation in fuel assemblies due to hydraulic forces. This involves assessing the distance at which the thickness variation of a water gap ceases to have a significant influence on hydraulic forces. In continuation, we address in the same section a study on the linearity of the hydraulic force given by our hydraulic model. This investigation aims to select a surrogate model that can adequately represent the hydraulic model within a coupling context. Section 3 marks a turning point towards the development of a methodology dedicated to the sensitivity analysis (Saltelli et al., 2004) of the hydraulic model. We intend to explore the range of deformations, ranging from small to large values, with the aim of creating a surrogate model, suitable for coupling with mechanics, using the Gaussian process technique presented in Rasmussen and Williams (2006). The focus will be on developing a robust approach to identify key parameters of the hydraulic model that most significantly influence fuel assembly deformations.

In summary, this article aims to provide a comprehensive overview of the relationship between assembly deformations and hydraulic forces estimated by a dedicated tool. Through the analysis of deformation propagation, characterization of the linearity of the hydraulic force model, and the development of a sensitivity analysis methodology, we seek to create relevant statistical tools for subsequent applications, particularly uncertainties quantification of the simulation of fuel assembly bow involving a coupling with mechanics.

2. Preliminary study of hydraulic contribution

Hydraulic forces play a crucial role in the deformation of fuel assemblies, resulting from complex phenomena occurring within the reactor core. Among these phenomena, macroscopic flow redistribution are induced by differences in behavior between the inlet and outlet. Furthermore, local-scale redistribution are observed, such as significant redistribution upstream of the grids. The grids of the fuel assemblies exert a significant influence on the flow within the reactor. When the assembly undergoes deformation, the dimensions of the spaces between the grids are affected. This variation affects the flow distribution between the grids, leading to disparities in pressure applied to the opposite outer sides of the same grid (see Fig. 3). Consequently, forces applying on the grids, along with the ones applying on the fuel assembly bundles, both contribute to the lateral deformation of the assembly.

The main objective of the flow models focusing on hydraulic network (de Lambert et al., 2021) is to characterize the flow existing between two adjacent grids by modeling it using the extended Bernoulli's equation. Considering a streamline [AB], the relation between the flow velocity and pressure is given by:

$$P_A + \frac{1}{2}\rho V_A^2 = P_B + \frac{1}{2}\rho V_B^2 + \Delta P \tag{1}$$

where P represents the pressure, V the bulk velocity, ΔP the irreversible pressure loss between A and B, where ΔP is generally written as $\Delta P = KQ^{\alpha}$ with the exponent α depending on the formula used, K the hydraulic resistance coefficient, and Q the volumetric flow rate. Consequently, in-core flow redistribution can be modeled with a pipe hydraulic network. All hydraulic simulations presented in this paper were calculated using a tool called Phorcys. The latter is used for evaluating the redistribution of volumetric flow rates in hydraulic networks (for more details, we refer to De lambert des champs de morel (2021)).

For the hydraulic code Phorcys, a number of input data exhibit uncertainty, whether it is of epistemic nature (resulting from a lack of knowledge or information) or stochastic nature (stemming from natural fluctuations of certain phenomena). To grasp this uncertainty, a multi-step methodology has been developed to study the use of the aforementioned code in our context. The validation of the code itself and the models used in this work, well beyond the scope of this article, is mainly based at the moment on the grid and fuel assembly local scales through comparison with simplified CFD simulations and experimental setups (de Lambert et al., 2021, 2023). This article focuses on the scale of a row of 15 fuel assemblies, in this case only qualitative comparisons can be performed with results in the literature.

The objective of this initial study is to assess the spatial propagation in Phorcys results due to a local perturbation of input parameters. This involves determining the distance at which the variation in thickness of a water gap, represented by λ, ceases to have a significant influence on hydraulic forces. Secondly, the aim is to evaluate the level of non-linearity between this local perturbation (λ) and its effect (force). These

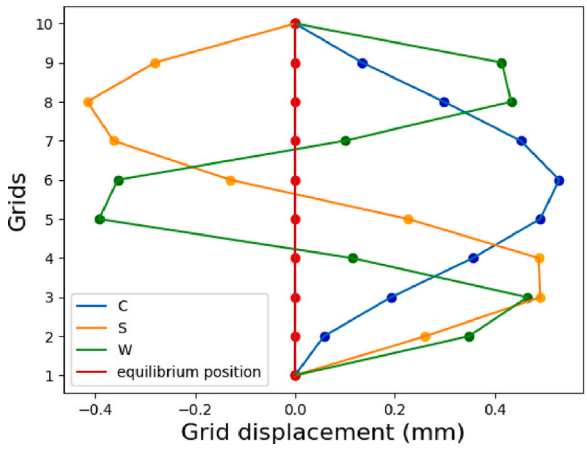

Fig. 4. Representation of the 3 deformation modes C, S, W.

objectives are geared towards establishing an appropriate method for conducting an initial sensitivity analysis.

2.1. Dimension reduction applied to the description of the deformed core

The methodology adopted in this study is applied on a row of 15 assemblies. We aim at better understanding the effect of perturbing a specific assembly in this row. The objective is to measure the decrease in perturbed hydraulic forces as a function of distance (assembly position). To simplify the complexity, a dimensional reduction on the assembly deformation is performed by representing the displacements of the 10 grids within an assembly using only 3 carefully chosen modes, denoted as C, S, W (Franzen, 2017) (see Fig. 4). Subsequently, the fields of hydraulic forces resulting from the deformed mode are compared to those of the undeformed mode (straight assembly) $\Delta F_h = F_h(deformed) - F_h(straight)$, where the force considered, F_h, is the total lateral hydraulic force at a given assembly span (grid + bundle) centered on one grid (see de Lambert et al., 2023). This comparison will assess the impact of the various deformation modes on hydraulic forces.

2.2. Choice of boundary conditions

The hydraulic models used (see Figs. 6 and 7) require to impose flow profiles at both the core inlet and outlet. In total 4 profiles have been considered in our study: Horvath (Horváth and Dressel, 2013), parabolic, homogeneous, and offset (see Fig. 5). In all cases the order of magnitude of the flow velocity is around 5 m/s. The results obtained are presented in the form of perturbations, where ΔF_h represents the force perturbation related to local bow perturbation considering initially straight assemblies. This approach allows us to assess the influence of different velocities and deformation conditions on hydraulic forces.

2.3. The impact of a fuel assembly deformation on hydraulic forces

In this section, we present the results of lateral hydraulic force variation due to the deformation of a single fuel assembly located in the middle of row A_8 and two neighboring assemblies A_8 and A_9 simultaneously, also positioned in the middle. One can note that calculations were performed using different velocity profiles for all three deformation modes, and specific studies were undertaken regarding fuel assemblies close to the periphery of the core (A_2, A_3) and (A_{13}, A_{14}). However, we only present the results obtained with the Horvath profile (Horváth and Dressel, 2013), which is an illustrative case, and the deformation mode C (see Figs. 6 and 7).

The presented results clearly show that the deformation of an assembly mainly affects the hydraulic forces on the assembly itself as well as on its nearest neighbors. This observation holds true for all velocity profiles mentioned earlier and also for all deformation modes in the case of small deformations, i.e. when the maximum amplitude of the mode is less than or equal to 2 mm, which is the nominal value considered for the water gap (distance between 2 grids).

2.4. Study of the linearity of the hydraulic model

After a first study on small perturbations propagation, in order to choose the most appropriate method to construct a surrogate model that could be used in a future work (for instance propagation of uncertainties during a fluid–structure coupling of 15 assemblies), it is interesting to study the behavior of hydraulic forces in relation to the deformations of fuel assemblies. To achieve this, several studies have been conducted, and we detail them in this section.

Case of small deformations. In this paragraph, we address the case of small deformations, which represent a realistic scenario for new assemblies that are still slightly deformed. Small deformations are characterized by water gap thicknesses close to 2 mm and the absence of contact between the assemblies. Three studies were conducted to test the linearity of hydraulic forces output: The first study is to test local linearity on an assembly, to verify if $\Delta F_h(K.\mathrm{Mod}_i(A_8)) = K.\Delta F_h(\mathrm{Mod}_i(A_8))$, the second one is to test the linearity of the linear combination of $(C + S + W)$ and $(C + S - W)$ on an assembly $(\Delta F_h(K.\Sigma\mathrm{Mod}_i(A_8)) = K.\Sigma(\Delta F_h(\mathrm{Mod}_i(A_8)))$, and the third study is to test a simultaneous perturbation of the assemblies (A_8 and A_9) $(\Delta F_h(K.\Sigma\mathrm{Mod}_i(A_8 + A_9)) = K.\Sigma(\Delta F_h(\mathrm{Mod}_i(A_8 + A_9)))$. All cases have been tested, and we will present the case of the linear combination of the 3 deformation modes on a single assembly A_8, namely $(C+S+W)$ (Fig. 8), subject to parabolic boundary conditions, since the results of all our tests were similar.

According to the results in Fig. 9, one can observe the linearity of hydraulic forces in relation to the amplitude of deformation in the case of small deformations. It is noteworthy that this linearity is generally preserved even in the case of a heterogeneous and off-centered flow that was tested. These findings are important as they provide valuable information to guide metamodelling and facilitate the understanding of hydraulic forces in real conditions where the flow can be heterogeneous and off-centered.

Case of large central water gaps. Now, we focus on the case of a strongly deformed barrel-shaped core, meaning with a water gap of about 10 to 20 mm at the center of the core, and consequently, a majority of assemblies deformed on either side (see Fig. 10). This geometric configuration is commonly observed at the end of power cycles (which last approximately one year). To do this, we will consider different values of central water gaps, namely 5, 10, 15, and 20 mm, and analyze the corresponding response of hydraulic forces.

We clearly observe a loss of linearity for a large water gap between 5 and 10 mm (see Fig. 11). The results obtained confirm that hydraulic forces do not follow a linear relationship beyond a certain value of the water gap. This loss of linearity is consistent with findings from DIVA+G experiments in Cardolaccia and de Lambert (2021). These observations highlight the importance of considering this non-linearity in hydraulic models. When water gaps exceed a certain value, it becomes necessary to use nonlinear approaches to accurately describe the behavior of hydraulic forces. These findings contribute to improving our understanding of the interactions between water gaps and hydraulic forces, providing valuable insights for the development of more precise surrogate models tailored to real conditions.

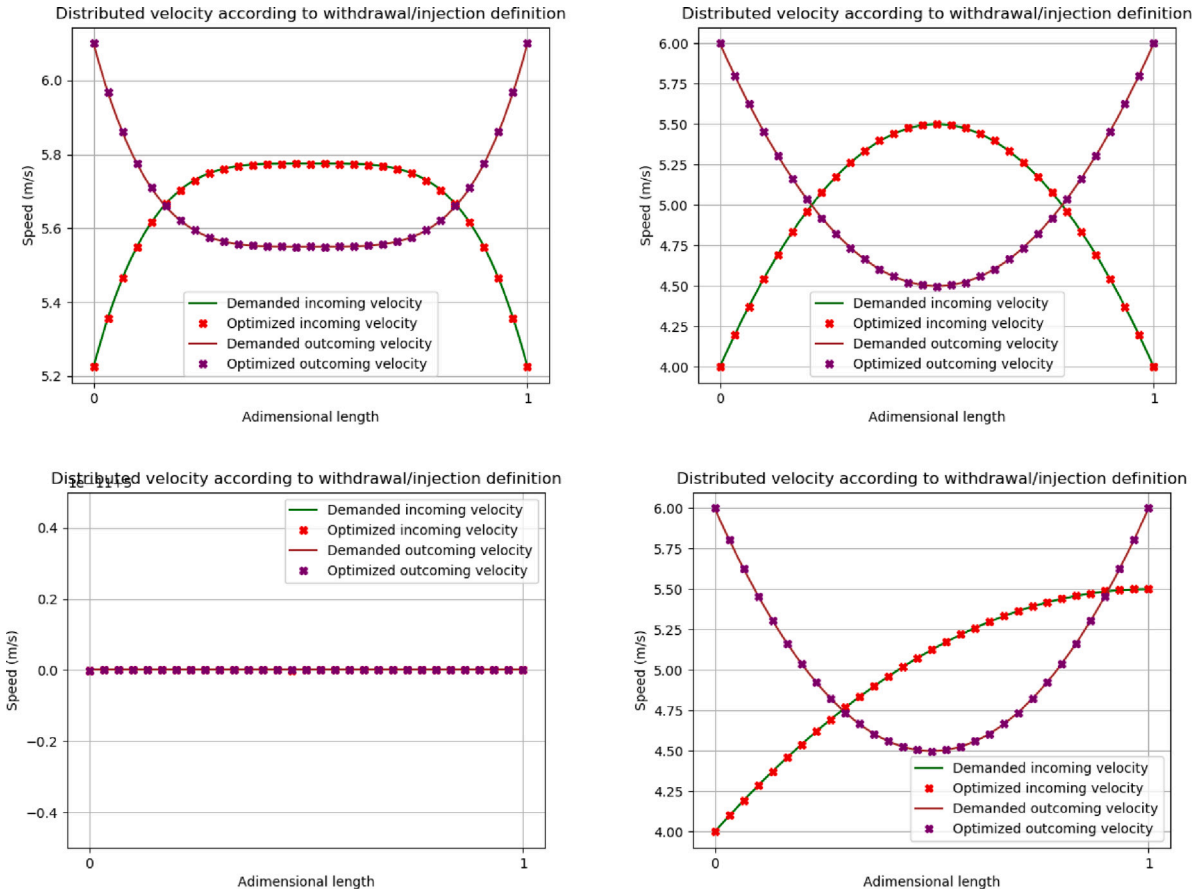

Fig. 5. Profiles: Horvath (top left), parabolic (top right), homogeneous (bottom left), and offset (bottom right). We note that the demanded profile is the one specified by the user, while the optimized profile is calculated by Phorcys for mass conservation.

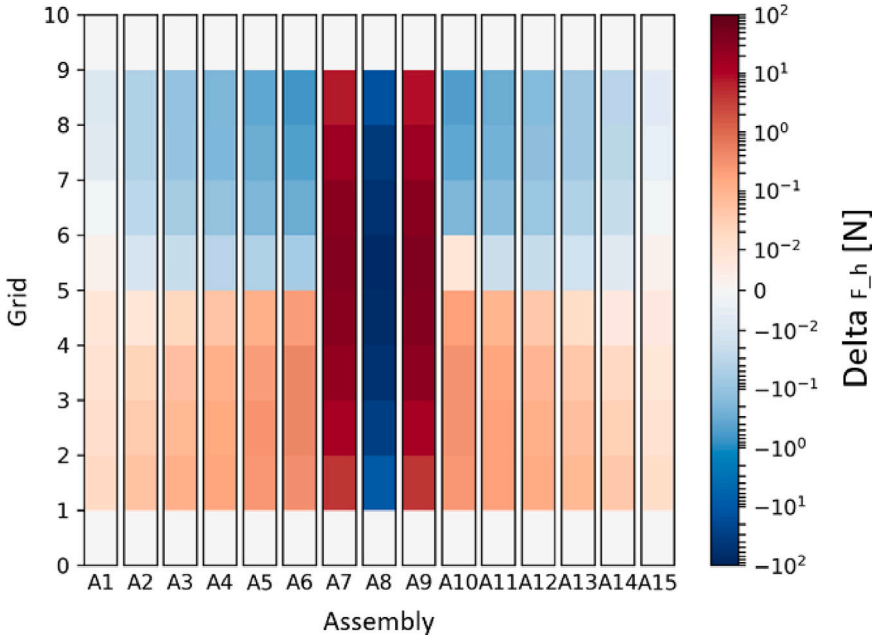

Fig. 6. Spatial distribution of ΔF_h after A_8 deformation.

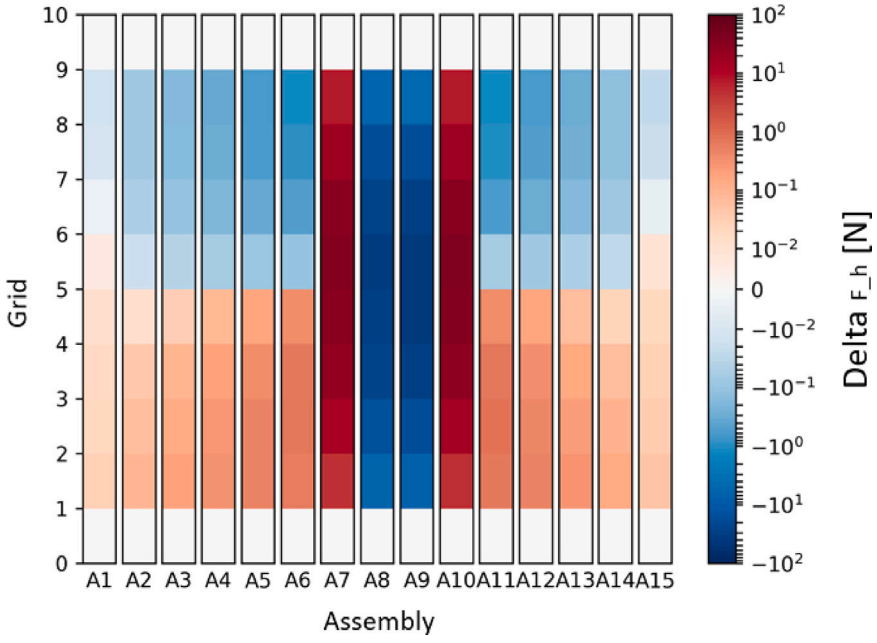

Fig. 7. Spatial distribution of ΔF_h after A_8 and A_9 deformation simultaneously.

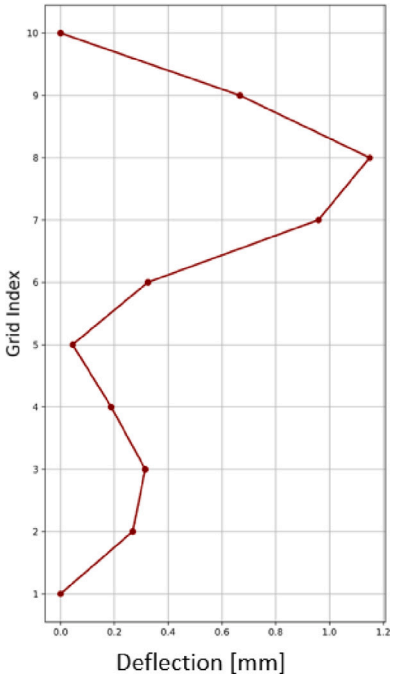

Fig. 8. Mode (C+S+W).

Conclusion. To conclude, concerning hydraulic forces contributing to the deformation of fuel assemblies, two distinct regimes can be identified based on the deformation level. In the regime of small deformations, hydraulic forces vary almost proportionally to deformations, and disturbances remain local. However, when examining the regime of large deformations, non-linearity is observed starting between 5 to 10 mm. To deepen our understanding of these phenomena, two orientations of sensitivity analysis have been considered. The first sensitivity analysis focuses on small deformations to assess their impact on hydraulic forces in the quasi-linear regime. The second sensitivity analysis, on the other hand, considers the case of large central water gaps where non-linearity is observed. These two orientations of sensitivity analysis will provide us with more detailed information about the behavior of hydraulic forces in different deformation regimes and quantify the uncertainty of the hydraulic models used with Phorcys.

3. Sensitivity analysis for hydraulic model

In this section, we perform a sensitivity analysis using the Sobol method (Sobol, 2001) for both deformation regimes, namely, small and large deformations of fuel assemblies. The goal is to investigate how the uncertainty in the model output can be distributed among the various sources of uncertainty in the input parameters of the model (Saltelli et al., 2004). We recall the definitions of the first-order and total Sobol indices. If $\mathbf{X} = (X^{(i)})_{i=1}^{d}$ is the vector of independent input parameters and Y is the scalar output, then

$$S_i = \frac{\mathrm{Var}(\mathbb{E}[Y|X^{(i)}])}{V}, \qquad T_i = \sum_{v \in \mathcal{P}, i \in v} S_v = 1 - \frac{\mathrm{Var}(\mathbb{E}[Y|\mathbf{X}^{(-i)}])}{V}, \tag{2}$$

where $V = \mathrm{Var}(Y)$, $\mathcal{P}$ is the set of subindices in $\{1, \dots, d\}$, $\mathbf{X}^{(-i)} = (X^{(1)}, \dots, X^{(i-1)}, X^{(i+1)}, \dots, X^{(p)})$, and S_v is the high-order Sobol index $S_v = \mathrm{Var}(\mathbb{E}[Y|\mathbf{X}^{(v)}])/V$ with $\mathbf{X}^{(v)} = (X^{(i)})_{i \in v}$. S_i is the first-order index that measures the contribution to the output variance of the main effect of the ith input alone. T_i is the total index that measures the contribution to the output variance of the ith input, including all variance caused by its interactions with any other input variables.

3.1. A first sensitivity analysis: Case of small deformations

Motivated by the previous results, an initial sensitivity analysis is conducted to assess the impact of small deformations in the hydraulic model, which provides the forces to be applied in the thermomechanical calculation. To conduct this analysis, it is essential to consider all uncertain parameters of the code and assign them an appropriate probability distribution based on reliable bibliographic references. The goal of this initial sensitivity analysis is to understand how small deformations, along with other parameters, influence the results of the hydraulic model. The calculations of Sobol indices are performed using the Uranie platform of CEA: an open-source software for optimization, meta-modeling and uncertainty analysis (Blanchard et al., 2019).

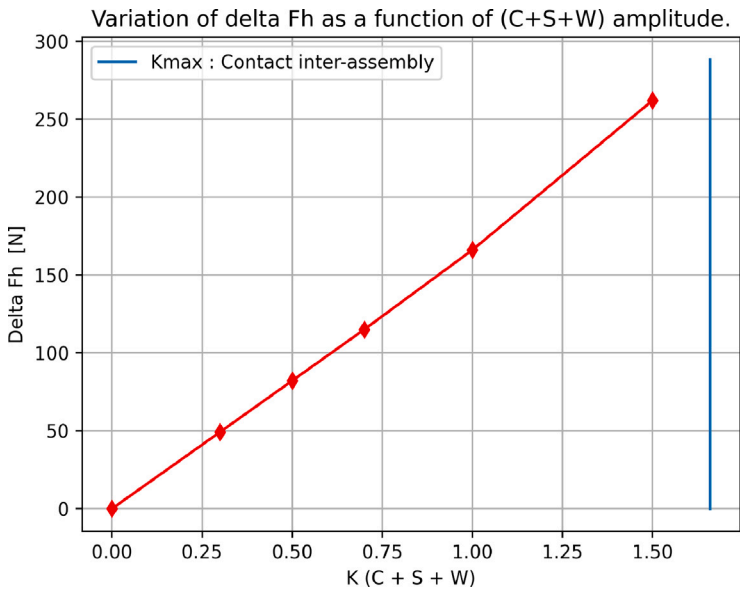

Fig. 9. Variation of ΔF_h of Grid 6 as a function of (C+S+W) amplitude.

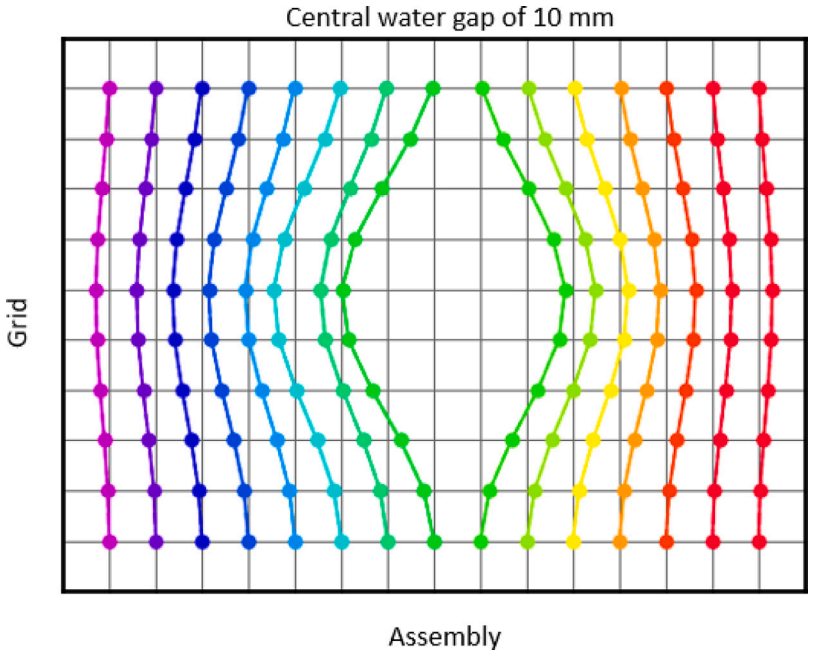

Fig. 10. Central water gap of 10 mm.

3.1.1. Uncertain parameters of the hydraulic model

Table 1 provides us with a definition of these parameters as well as the chosen probability distribution for each parameter, based on information from the cited references. V, M_{in}, L^{in}_{offset}, M_{out}, and L^{out}_{offset} are parameters that determine the boundary conditions at the inlet and outlet of the core.

h_l **parameter:** The model 3 presented in de Lambert et al. (2021), which includes a resistance to flow leakage, requires defining the parameter h_l, corresponding to the height used to calculate the lateral pressure drop ΔP_l. The example shown in de Lambert et al. (2021) demonstrates that the flow redistribution (from the bypass to the grids) starts at a distance h_l upstream of the grid. It has also been observed in this local model that when the value of h_l exceeds 30 mm, it does not affect the flow or the pressure drop, as a quasi-asymptotic regime is reached beyond this value (see DELAMBERT2021110940). However, there is a singular point when λ and h_l both approach 0, where the upstream pressure drop associated with flow redistribution becomes potentially infinite. This is logical since this singular point corresponds to a situation in which almost all incoming flow would be forced to pass through the grids ($\lambda = 0$) through an extremely narrow horizontal gap ($h_l = 0$). Therefore, it is important not to choose a value that is too small for this parameter. In conclusion, we opted for a uniform distribution for h_l, $h_l \sim \mathcal{U}(10, 30)$.

C_{ij} **the modal coefficients:** We chose to create an orthonormal family of 3 deformation modes, denoted as C, S, and W (see Fig. 4) to represent the deformation of each assembly by projecting the displacements onto these three modes. This enables us to represent the deformation of an assembly with only 3 amplitudes in the xoz plane and 3 other amplitudes in the yoz plane for a 3D calculation. This already leads to a significant dimensional reduction in describing the assemblies' deformations. Moreover, the water gaps (defined in

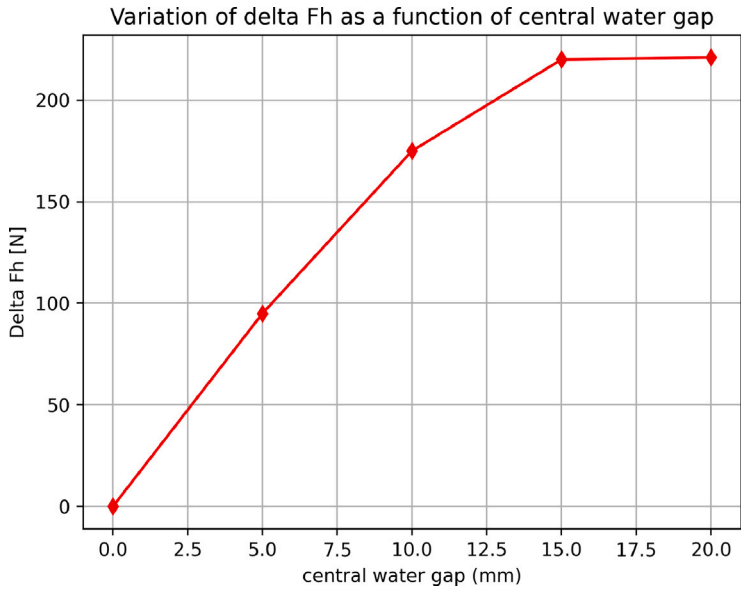

Fig. 11. Variation of ΔF_h of Grid 6 as a function of the central water gap.

Table 1
Table of uncertain input parameters and their probability distributions.

Parameter	Definition	Distribution
C_{ij}	Modal coefficients	$\mathcal{N}\left(\mathbf{0}, \sigma_i^2 \mathbf{M}\right)$ [3.1.1]
T (°C)	Temperature	$\mathcal{N}(\mu = 300, \sigma^2 = 11.08)$ (Jang et al., 2021)
h_l (mm)	Redistributing flow height	$\mathcal{U}(10, 30)$ (de Lambert et al., 2021)
C_g	Axial loss coefficient for a grid	$\mathcal{U}(1, 1.22)$ (In et al., 2002)
M_{in}	Flattening of the parabolic incoming velocity profile	$\mathcal{N}(\mu = 0.05, \sigma^2 = 0.005^2)$ (Sheng and Seidl, 2015; Wanninger, 2018)
V (m/s)	Flow velocity	$\mathcal{N}(\mu = 5, \sigma^2 = 0.05^2)$ (De lambert des champs de morel, 2021)
$L^{in}_{of\,fset}$	Offsetting of the parabolic incoming velocity profile	$\mathcal{N}(\mu = 0, \sigma^2 = 0.2^2)$ (Sheng and Seidl, 2015; Wanninger, 2018)
M_{out}	Flattening of the parabolic outgoing velocity profile	$\mathcal{N}(\mu = 0.04, \sigma^2 = 0.004^2)$ (Sheng and Seidl, 2015; Wanninger, 2018)
$L^{out}_{of\,fset}$	Offsetting of the parabolic outgoing velocity profile	$\mathcal{N}(\mu = 0, \sigma^2 = 0.1^2)$ (Sheng and Seidl, 2015; Wanninger, 2018)

Section 2) can also be expressed in this same family as they are algebraically derived from the assemblies' deformation. Initially, we aim to conduct an initial sensitivity analysis using a row of 15 assemblies. As already demonstrated, the water gaps λ are expressed in terms of the modes C, S, and W as follows: $\lambda_j(z) = \sum_{i=1}^{3} C_{ij} f_i(z) + \lambda_0$, where i is the mode index, $j = 1, \ldots, n_\lambda = 16$ is the index of the water gap, C_{ij} represents the modal coefficient, $f_i(z)$ corresponds to the lateral displacement mode of the assembly expressed in terms of heights z of all grids: $z = 1, \ldots, 10$. $\lambda_0 = 2$ mm is the nominal value of λ (in the case of undistorted assemblies). As the core is constructed in an axisymmetric manner, the C_{ij} can be positive or negative depending on the direction of movement. We choose each C_{ij} to follow a normal distribution with zero mean and standard deviation σ ($C_{ij} \sim \mathcal{N}(\mu = 0, \sigma)$). First, there are two physical conditions to verify: the **inter-assembly non-penetration constraint** and the **conservation of the total distance**. In the case of small disturbances in the water gaps, the first constraint will be automatically satisfied. As for the second constraint, considering that the assemblies are placed inside the vessel, which has a constant diameter, and are uniformly distributed over the total distance of the vessel with a nominal gap of $\lambda_0 = 2$ mm between assemblies and between peripheral assemblies and the vessel, for undeformed assemblies, this implies that for a row of 15 assemblies, the total clearance is equal to $n_\lambda . \lambda_0 = 32$ mm. These constraints can be expressed after projection onto the family of the three modes as follows. The first constraint is $\sum_{i=1}^{3} C_{ij} f_i(z) + \lambda_0 \geq 0 \ \forall j, z$, and the second one is $\sum_{j=1}^{n_\lambda} \sum_{i=1}^{3} (C_{ij} f_i(z) + \lambda_0) = n_\lambda \lambda_0 \ \forall z$. It is deduced that to verify the constraint of total distance conservation, it is necessary to condition by $\sum_{j=1}^{n_\lambda} C_{ij} = 0$ for all i. To do this, we use Theorem of Gaussian conditioning. Denoting $\boldsymbol{Y}_1 = (C_i)_{i=1}^{n_\lambda}$ and $Y_2 = \sum_{j=1}^{n_\lambda} C_j$, the distribution of $\boldsymbol{Y}_1$ given $Y_2 = y_2$ is

$$\mathcal{L}\left(\boldsymbol{Y}_1 \mid Y_2 = y_2\right) = \mathcal{N}\left(\mathbf{R}_{12} R_{22}^{-1} y_2, \mathbf{R}_{11} - \mathbf{R}_{12} R_{22}^{-1} \mathbf{R}_{21}\right),$$

with $\mathbf{R}_{11} = \sigma^2 \mathbf{I}$ where $\mathbf{I}$ the $n_\lambda \times n_\lambda$ identity matrix, $\mathbf{R}_{12} = \sigma^2 (1, \ldots, 1)^T$, $\mathbf{R}_{21} = \mathbf{R}_{12}^T$, $R_{22} = n_\lambda \sigma^2$. With $y_2 = 0$, we can conclude that :

$$\mathcal{L}\left(\boldsymbol{Y}_1 \mid Y_2 = 0\right) = \mathcal{N}\left(\mu', \Sigma'\right) \text{ with } \mu' = (0, \ldots, 0)^T \text{ of size } n_\lambda, \ \Sigma' = \sigma^2 \mathbf{M}$$

with $\mathbf{M} = \mathbf{I} - n_\lambda^{-1} \mathbf{U}$ and $\mathbf{U}$ the $n_\lambda \times n_\lambda$ matrix full of ones. It is noted that the variance of the coefficients C_i after conditioning is $\sigma^2(1 - 1/n_\lambda)$. If this is the value to be imposed, then σ^2 should be taken equal to this value divided by $1 - 1/n_\lambda$.

We also know that modes S and especially W always have amplitudes lower than that of mode C. Therefore, it suffices to choose a standard deviation σ_c for $C_j(c)$ larger than σ_s and σ_w for $C_j(s)$ and $C_j(w)$. This strategy allows us to conduct an initial sensitivity analysis with the 3 independent vectors:

- $C = C_{1j} \sim \mathcal{N}\left(\mu_c, \Sigma_c\right)$ avec : $\mu_c = (0, \ldots, 0)^T$ of size $n = 16$, $\Sigma_c = \sigma_c^2 \mathbf{M}$.
- $S = C_{2j} \sim \mathcal{N}\left(\mu_s, \Sigma_s\right)$ avec : $\mu_s = (0, \ldots, 0)^T$ of size $n = 16$, $\Sigma_s = \sigma_s^2 \mathbf{M}$.
- $W = C_{3j} \sim \mathcal{N}\left(\mu_w, \Sigma_w\right)$ avec : $\mu_w = (0, \ldots, 0)^T$ of size $n = 16$, $\Sigma_w = \sigma_w^2 \mathbf{M}$.

3.1.2. A sobol sensitivity analysis on the force at each grid level

To give a physical meaning to our study, we decided to perform a Sobol sensitivity analysis for each grid in the row of 15 assemblies. We

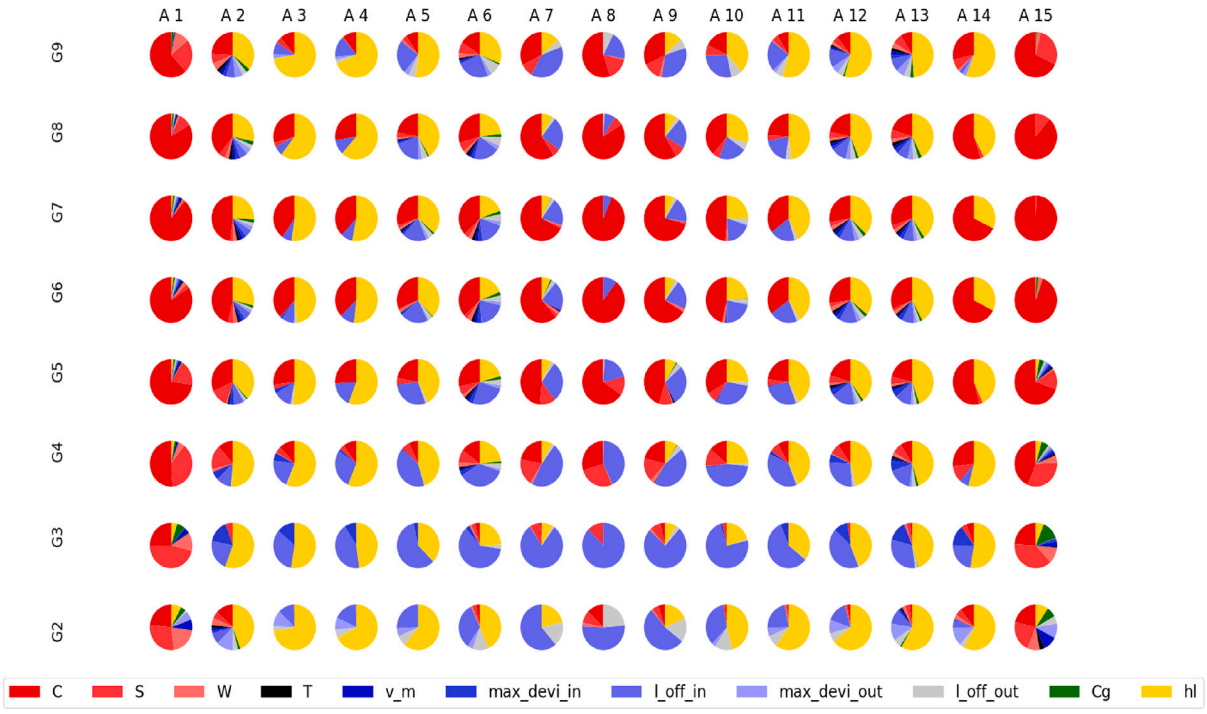

Fig. 12. Spatial distribution of first-order Sobol indices for evaluating lateral force at each grid level.

choose total hydraulic force centered on each grid (F_h) as the quantity of interest to observe the spatial variation of dependencies. We only present the results for grids 2 to 9, as grids 1 and 10 are fixed. We find that the Sobol indices for hydraulic forces at each grid level for both first-order and total effects are almost equal. This allows us to conclude that there is small interaction between the parameters. Therefore, we present the results of the first-order Sobol indices at each grid level. The results are presented in the form of circular diagrams (see Fig. 12) to provide an idea of the most influential parameters at each grid level for each assembly.

Analysis of the results: In this analysis on the hydraulic forces at different grid levels (from height 2 to height 9), the results indicate that the most influential parameters vary with height. At grid levels 2 to 4, hydraulic forces are primarily influenced by the offset of the velocity profile parabola (L^{in}_{offset}) and the epistemic parameter h_l, as deformations are negligible in these regions. As the observation moves up to grids 5 to 8, the deformation mode C becomes the most influential parameter, closely followed by h_l. Mode C exhibits higher amplitudes and dominates at grid level 6. Deformation modes S and W also influence areas where their amplitudes are maximal. Finally, at grid level 9 near the upper plenum, the epistemic parameter h_l along with velocity profile parameters become dominant. For peripheral assemblies, deformations remain the most influential parameters.

After calculating the Sobol indices, we also present the spatial distribution of standard deviations across a series of 15 assemblies (see Fig. 13) to identify locations where they are high. According to the obtained results, it is evident that the greatest dispersion is observed at grid levels 5 and 6, where the amplitude of mode C is maximal, also the distribution along the horizontal axis follows a distribution of forces in an undeformed case without boundary offset. These findings align with those obtained during the Sobol analysis.

Conclusion : This study enabled us to examine the spatial distribution of the Sobol indices in great detail. This enabled us to observe, in a very local and precise way, what is happening at the level of each grid of the 15 assemblies, and to classify the most influential parameters for each grid of each assembly. In addition, we were able to adopt a more global perspective by examining all the grids at the same height, which enabled us to analyze the results at the entry, within and exit of the core, and to identify the most influential parameters on the hydraulic forces. In summary, we found the significant effect of the boundary conditions at the core inlet and outlet, which, in the absence of any deformation of the assemblies, are the main cause of the velocity gradients, which in turn create the hydraulic forces. It is worth highlighting the remarkable influence of the epistemic parameter h_l, which always remains influential and comparable to that of small deformations for non-peripheral assemblies.

3.2. A second sensitivity analysis: Case of large deformations

In this section, we focus on the sensitivity analysis of the hydraulic model in the context of large deformations. To achieve this, we apply a deformation of 20 mm (see Fig. 14) between A_8 and A_9, with the aim of identifying the epistemic and stochastic parameters that exert the greatest influence on the hydraulic forces. Since the deformation has been fixed, this results in the absence of modal coefficients C_{ij}.

According to the results shown in Fig. 15, it is evident that the influence of hydraulic boundary conditions becomes particularly significant on grids 4 to 7, where the largest water gaps are generated. These wide gaps then strongly affect flow redistribution, consequently, the calculation of hydraulic forces. This observation highlights the crucial role of boundary conditions in such regions. In these same areas, the epistemic parameter h_l also consistently emerges as a dominant factor. These findings align with our previous analysis: in the absence of assembly deformation, hydraulic forces are mainly induced by velocity gradients induced by the boundary profiles. Furthermore, in regions of pronounced transverse flows — particularly where assemblies are in contact or nearly touching h_l maintains its dominant influence. Overall, in the large deformation regime, h_l remains the most influential parameter, followed closely by the boundary conditions, particularly the parameter L^{in}_{offset}.

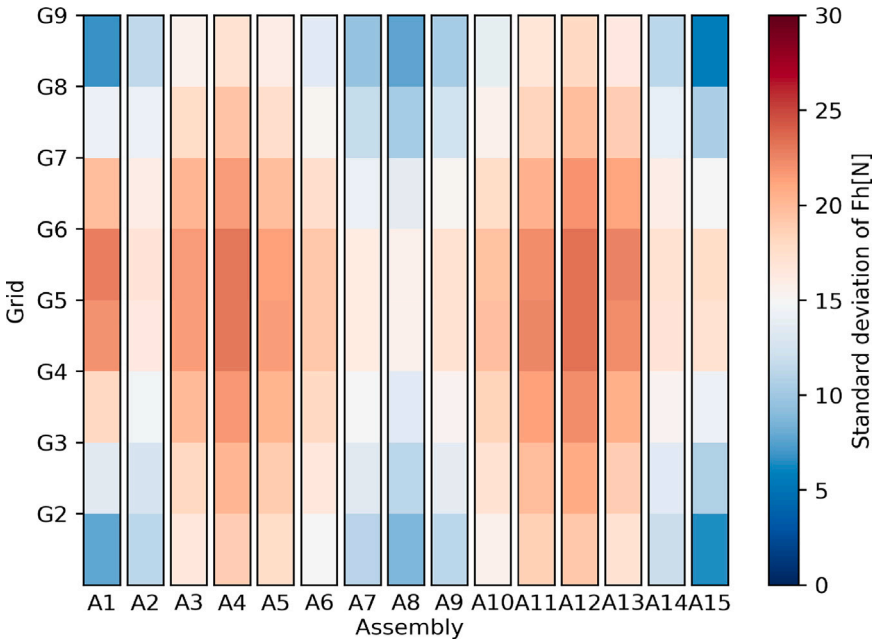

Fig. 13. Spatial distribution of the standard deviation of F_h.

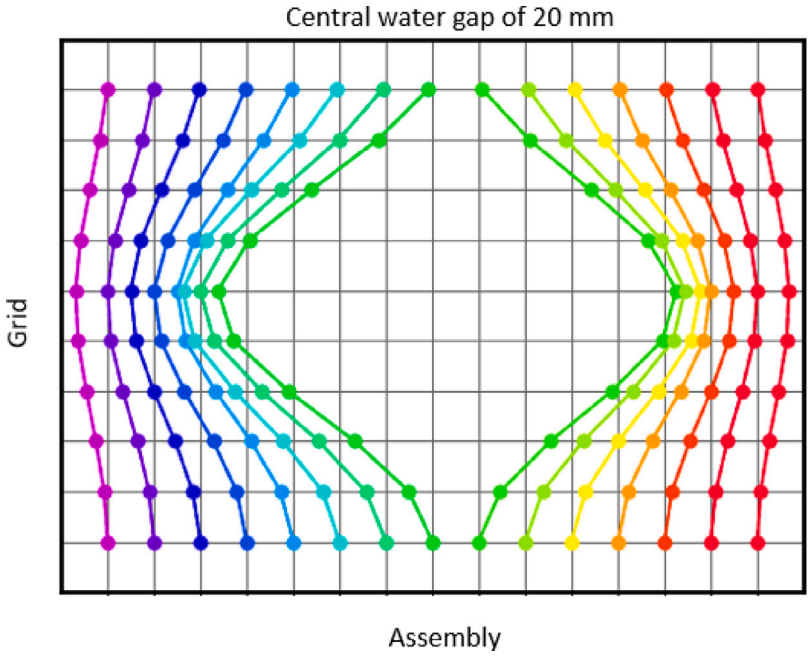

Fig. 14. 20 mm water gap imposed for the sensitivity analysis.

We then decided to present the spatial distribution of standard deviations over a series of 15 assemblies (see Fig. 16) to identify the locations where these deviations are the highest. It is clearly observable that the maximum standard deviation values are located in the middle zone of the 15 assemblies, where we applied our large deformation. This analysis shows that the variance of hydraulic forces increases in the case of a significant water gap.

4. Surrogate modeling of hydraulic model using Gaussian process

The previous studies extended our understanding of hydraulic forces both in terms of behavior and parameters influence. On the one hand, it gives important information on the models, on the other hand, it helps to better setting up surrogate models. Indeed, in the context of propagating uncertainties at the core level, a methodology of a future work could consist in using surrogate models instead of codes. In this section we present a first surrogate model for hydraulic forces in the case of small deformations. The latter must be rightly selected. An accurate metamodel is also necessary to carry out uncertainty quantification and quantitative sensitivity analysis (such as Sobol' method Sobol, 2001). Motivated by the need to quantify the uncertainties, we have chosen to build Gaussian process metamodels.

Since the hydraulic model in the case of small deformations shows no particular irregularities, we have chosen to use the tensorized Matérn covariance kernel with the parameter $\nu = 3/2$. Considering the quasi-linear nature of the hydraulic forces model under the case of investigation, we decided to adopt a linear trend for the Gaussian

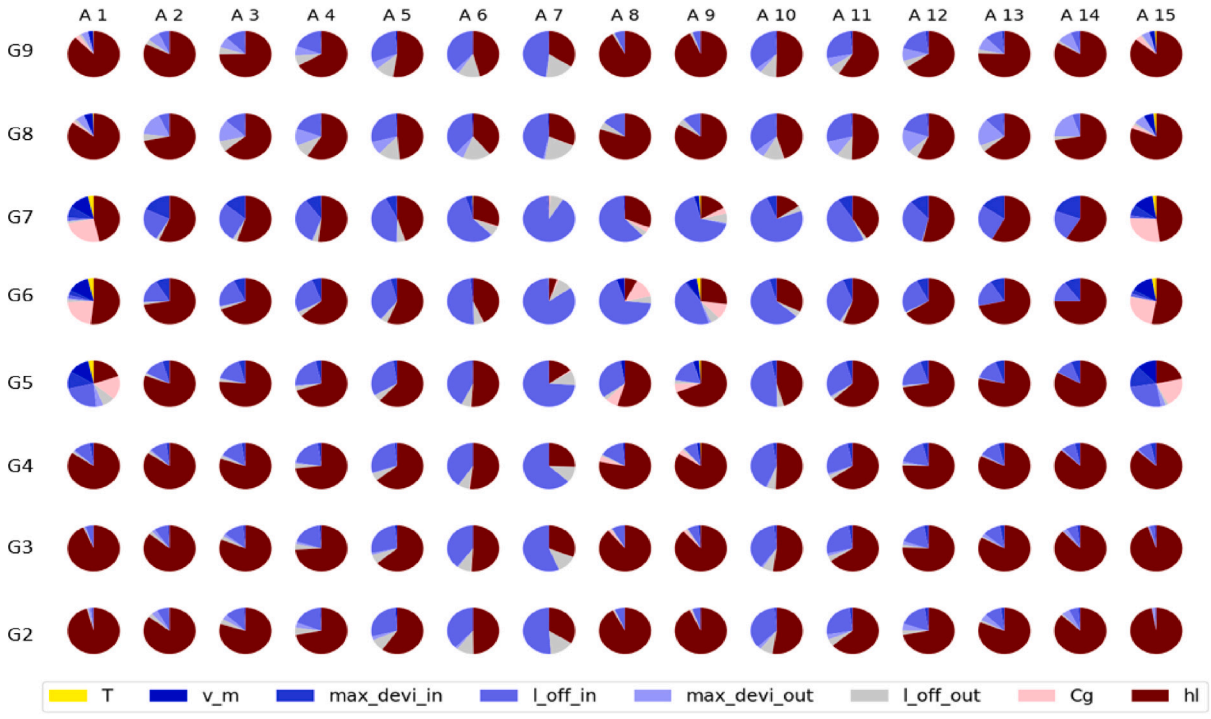

Fig. 15. Spatial distribution of first-order Sobol indices for evaluating lateral force at each grid level.

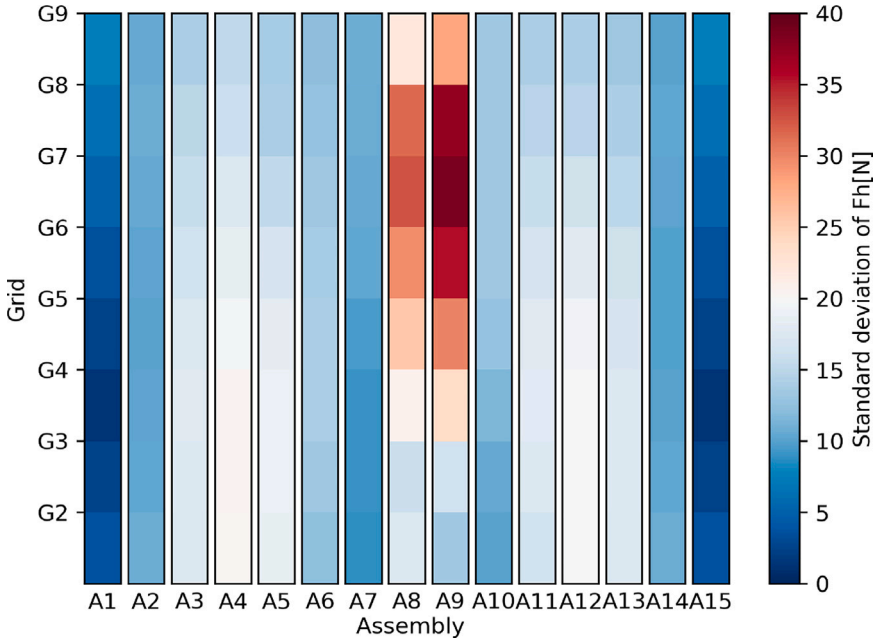

Fig. 16. Spatial distribution of the standard deviation of F_h.

process. The outputs of interest in our study are the same hydraulic forces as used before at each grid level. To assess the performance of our model, we calculate a Gaussian process for each scalar output.

This measure provides valuable insights into the quality of the model predictions for the force at each grid level. Regarding the estimation of the model's hyperparameters (variance and scalelengths), we opted for the Leave-One-Out (LOO) method (Blanchard et al., 2019). In Fig. 17 we present the spatial distribution of the factor Q^2, also known as the predictivity coefficient. It is estimated using a test dataset, denoted as $\mathcal{P} = \{(x^{(j)}, y^{(j)}) : j = 1, \dots, n_p\}$, consisting in n_p realizations distinct from the training dataset. It is calculated using the formula:

$$Q^2 = 1 - \frac{\sum_{j=1}^{n_p} \left(y^{(j)} - \hat{y}\left(\mathbf{x}^{(j)}\right)\right)^2}{\sum_{j=1}^{n_p} \left(y^{(j)} - \bar{y}_{test}\right)^2}, \quad \mathbf{x}^{(j)} \in \mathcal{P} \tag{3}$$

where $\bar{y}_{test}$ is the mean of the quantity of interest in the test basis, $y^{(j)}$ is the observed value, and $\hat{y}(\mathbf{x}^{(j)})$ is the predicted value.

We notice that the quality factors for the Gaussian processes at all grid levels are greater than 0.8. Moreover, the overall average value of

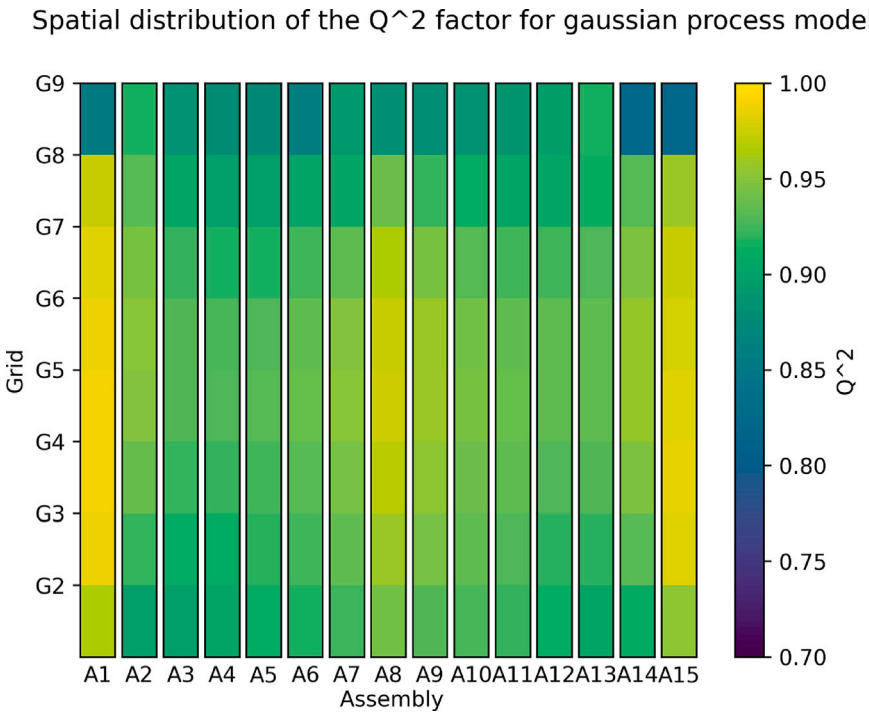

Fig. 17. Spatial distribution of the Q^2 factor for the Gaussian process model.

$Q^2 = 0.93$ confirms the predictive efficiency of the Gaussian process, thus validating its large-scale use.

In Fig. 18, through the standard deviation spatial distribution, we get a quantitative evaluation of the possible error using such a metamodel. The maximum value of about 6 N for a grid stage seems acceptable compared to the maximum forces that are commonly evaluated, reaching 100 N and more. It is also interesting to notice that the central and external regions exhibit very low prediction errors. This quality of prediction relative to the reference simulation for fluid forces is especially important for the very central fuel assemblies. Indeed, at the start of a new power cycle, the central assembly in the row is located in the core symmetry plane and is therefore close to the flow symmetry plane. As a result, it is generally subject to low lateral forces. However, it is precisely the sign of these low forces that must be carefully controlled, as they determine whether the assembly will move to the left or the right, thereby influencing the development of the core's deformation pattern. According to this reasoning, the moderate uncertainty in the calculated forces on the central assembly (Fig. 13), along with the surrogate model error as low as 3 N in this area (Fig. 18), are reassuring points with respect to the precision required for the mechanical calculation of deformations.

In conclusion, surrogate modeling by Gaussian process regression has proven effective in predicting hydraulic force at each grid level. We successfully represented hydraulic forces on each grid using a Gaussian process, establishing a reliable and accurate surrogate model within the regime of small deformations. For the purpose of uncertainty propagation over cycles, this surrogate will cover the inputs of deformation, hydraulic boundary conditions and epistemic parameters.

5. Conclusion

This article presents a comprehensive analysis of uncertainty in the simulation of lateral hydraulic forces, focusing on the hydraulic code *Phorcys*. Section 2 identifies two behavior regimes: linear lateral forces for small deformations and nonlinear forces for values of water gaps starting from 5 mm. A Sobol sensitivity analysis in Section 3 reveals the predominant influence of deformation mode C of the assembly bow and the epistemic parameter h_l, as well as the significant impact of flow boundary conditions. The spatial study of Sobol indices established for each grid in a row of 15 fuel assemblies confirms these findings, emphasizing the importance of h_l and flow boundary conditions. The results of this analysis give us two major directions for significantly improving the calculation of hydraulic forces exerted on fuel assemblies. The first would consist in no longer arbitrarily fixing the epistemic h_l parameter, but rather making it depend locally on the width of the water gap. The second direction would be to better take into account hydraulic boundary conditions rather than simply imposing flow profiles. This would involve, for instance, considering the intricate coupling between in-core flow and both inlet and outlet flows associated to plenums. Reversely, with regard to the design of future reactors, this sensitivity study highlights the influence of coolant velocity profiles upstream and downstream of fuel assemblies, and therefore the role of the geometry of the upper and lower plenums on FA bow.

In Section 4, taking advantage of the regularity of the phenomena involved in small deformations, it was shown that a Gaussian process surrogate model provides a very good prediction of lateral hydraulic forces. This means that such a surrogate model could be used in the coupled hydro-mechanical simulation in partial or complete replacement of the original hydraulic code at least in the case of small deformations.

Similar sensitivity analysis and metamodeling work is currently underway for the thermomechanical simulation of assembly bow in a PWR core. Ultimately, the numerical coupling of these two surrogate models, which benefit from an error estimator, should permit the joint analysis of sensitivities of the coupled hydraulic and mechanical simulations. This, in turn, will provide useful information on the accuracy of the results as well as on the areas of progress to be prioritized in order to further improve the quality of deformation prediction at the end of the irradiation cycle.

Ultimately, this work aims at a better understanding of the FA bow phenomenology as well as a more informed calculation of hydraulic forces within a core where fuel assemblies progressively deform due to fluid–structure interaction. In the long term, such knowledge and framework make it possible to evaluate fuel assembly performances efficiently and accurately. For instance, thanks to reduced computational costs, one can assess the long-term effect of different fuel management strategies, i.e. the choice of assembly permutations during

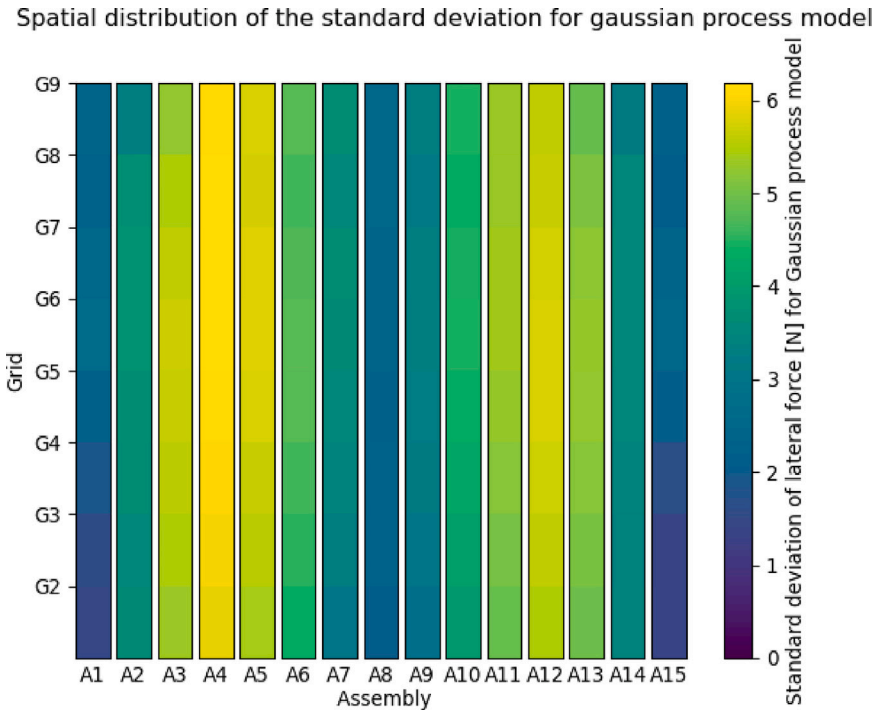

Fig. 18. Spatial distribution of the standard deviation of prediction for the Gaussian process model.

inter-cycle which conditions the initial state of deformation of the core at the beginning of each cycle. Similarly in the frame of optimizing fuel burn-up, a performant hydro-mechanical simulation enables to rank candidate fuel management strategies to maximize economic and guarantee safety while considering FA bow.

With regard to the design of future reactors, this sensitivity study once again highlights the influence of coolant velocity profiles upstream and downstream of fuel assemblies, and therefore the attention that needs to be paid to the geometry of the upper and lower plenums to ensure sufficient homogeneity and low variability of velocity profiles.

CRediT authorship contribution statement

Ali Abboud: Writing – review & editing, Writing – original draft, Visualization, Validation, Software, Methodology, Investigation, Formal analysis, Data curation, Conceptualization. **Stanislas de Lambert:** Validation, Supervision, Software, Methodology, Formal analysis. **Josselin Garnier:** Validation, Supervision, Project administration, Methodology. **Bertrand Leturcq:** Validation, Supervision, Software, Resources, Methodology, Formal analysis. **Nicolas Lamorte:** Validation, Supervision.

Declaration of competing interest

The authors declare that they have no known competing financial interests or personal relationships that could have appeared to influence the work reported in this paper.

Acknowledgments

We thank Julien Pacull and Jean-Baptiste Minne (Framatome) for the stimulating and useful discussions about fuel assembly bow. We also thank Fabrice Gaudier (CEA) for his support on the URANIE platform.

Data availability

Data will be made available on request.

References

Andersson, T., Almberger, J., Björnkvist, L., 2005. "A decade of assembly bow management at ringhals". In: IAEA-TECDOC-1454 Structural Behaviour of Fuel Assemblies for Water Cooled Reactors. IAEA, Vienna, Austria, pp. 129–136.

Blanchard, J.-B., Damblin, G., Martinez, J.-M., Arnaud, G., Gaudier, F., 2019. "The uranie platform: an open-source software for optimisation, meta-modelling and uncertainty analysis". EPJ N - Nucl. Sci. Technol. 5, 4.

Cardolaccia, J., de Lambert, S., 2021. "Investigation of the flow redistribution upstream of grid-like obstacles separated by a variable gap". Exp. Therm. Fluid Sci. 121, 110289.

Clouvel, L., 2019. "Uncertainty Quantification of the Fast Flux Calculation for a PWR Vessel" (Ph.D. thesis). (2019SACLS414), Université Paris Saclay (COmUE).

de Lambert, S., Cardolaccia, J., Faucher, V., Leturcq, B., Campioni, G., 2023. Semi-analytical fluid-structure model for the analysis of fuel assembly bow in full PWR cores. Prog. Nucl. Energy 160, 104668.

de Lambert, S., Cardolaccia, J., Faucher, V., Thomine, O., Leturcq, B., Campioni, G., 2021. Semi-analytical modeling of the flow redistribution upstream from the mixing grids in a context of nuclear fuel assembly bow. Nucl. Eng. Des. 371, 110940.

Franzen, A., 2017. "Evaluation of fuel assembly bow penalty peaking factors for ringhals 3 : Based on a cycle specific core water gap distribution". Upps. Univ. Appl. Nucl. Phys..

Horváth, A., Dressel, B., 2013. "On numerical simulation of fuel assembly bow in pressurized water reactors". Nucl. Eng. Des. 265, 814–825.

In, W.K., Oh, D.S., Chun, T.H., 2002. "Empirical and computational pressure drop correlations for pressurized water reactor fuel spacer grids". Nucl. Technol. 139 (1), 72–79.

Jang, J., Kong, C., Ebiwonjumi, B., Cherezov, A., Jo, Y., Lee, D., 2021. "Uncertainty quantification in decay heat calculation of spent nuclear fuel by STREAM/RAST-K". Nucl. Eng. Technol. 53 (9), 2803–2815.

Lamorte, N., de Montigny, E.M., Goreaud, N., Chazot, B., Marx, V., 2021. "Advanced predictive tool for fuel assembly bow design performance evaluations". Proc. TOP FUEL Conf..

Lascar, C., Champigny, J., Chatelain, A., Chazot, B., Goreaud, N., de Montigny, E.M., Pacull, J., Salaün, H., 2015. "Advanced predictive tool for fuel assembly bow based on a 3D coupled FSI approach". Proc. TOP FUEL Conf..

De lambert des champs de morel, S., 2021. Contribution to the Multiphysical Analysis of Fuel Assembly Bow (Ph.D. thesis). Thèse de doctorat dirigée par Faucher, Vincent-Campioni, Guillaume et Cardolaccia, Jérome Énergétique université Paris-Saclay 2021.

Pernice, M., 2012. Considerations for Sensitivity Analysis, Uncertainty Quantification, and Data Assimilation for Grid-To-Rod Fretting. Technical Report INL/EXT-2012-27267, Idaho National Laboratory, Idaho Falls, ID.

Rasmussen, C.E., Williams, C.K.I., 2006. "Gaussian Processes for Machine Learning", vol. 2, MIT Press, Cambridge, MA.

Roudier, S., Béraha, R., 1996. "Nuclear fuel in France: an ever changing world - most recent safety concerns of dsin". In: Specialist Meeting on Nuclear Fuel and Control Rods: Operating Experience, Design Evolution and Safety Aspects. OECD-NEA, Madrid, Spain, pp. 63–77.

RSK, 2015. "Verformungen von brennelementen in deutschen druckwasserreaktoren (DWR). RSK-stellungnahme". 474. Sitzung der Reaktor-Sicherheitskommission (RSK) am 18.03.2015.

Saltelli, A., Tarantola, S., Campolongo, F., Ratto, M., 2004. "Sensitivity analysis in practice: A guide to assessing scientific models".

Sheng, D.-Y., Seidl, M., 2015. Towards the development of a full-scale transient CFD model to simulate the static and dynamic in-core mass flux distribution in a classical german PWR. In: Proceedings of NURETH-16: 16th International Topical Meeting on Nuclear Reactor Thermal-Hydraulics. American Nuclear Society, Chicago, IL, USA, Westinghouse Electric Sweden AB (Västerås, Sweden); E.ON Kernkraft GmbH (Hannover, Germany); Correspondence: shengd@westinghouse.com, marcus.seidl@eon.com.

Sobol, I.M., 2001. Global sensitivity indices for nonlinear mathematical models and their Monte Carlo estimates. Math. Comput. Simulation 55 (1–3), 271–280.

Wanninger, A., 2018. Mechanical Analysis of the Bow Deformation of Fuel Assemblies in a Pressurized Water Reactor Core (Ph.D. thesis). Technische Universität München, Munich, Germany, Vollständiger Abdruck der von der Fakultät für Maschinenwesen der Technischen Universität München zur Erlangung des akademischen Grades eines Doktor-Ingenieurs (Dr.-Ing.) genehmigten Dissertation.